H, Takayama K, Tamakawa Y, Yanagisawa T, Fujiwara A and Mitoya K: High-speed soft x-ray generators in biomedicine. *SPIE*, 2513:649-667, 1994.

9) Sato E, Sagae M, Takahashi K, Shikoda A, Oizumi T, Ojima H, Takayama K, Tamakawa Y, Yanagisawa T, Fujiwara A and Mitoya K: Dual energy flash x-ray generator, *SPIE*, 2513:723-735, 1994.

10) Shikoda A, Sato E, Sagae M, Oizumi T, Tamakawa Y and Yanagisawa T: Repetitive flash x-ray generator having a high-durability diode driven by a two-cable-type line pulser. *Rev. Sci. Instrum.*, 65: 850-856, 1994.

11) Sato E, Takahashi K, Sagae M, Kimura S, Oizumi T, Hayasi Y, Tamakawa Y and Yanagisawa T: Sub-kilohertz flash x-ray generator utilizing a glass-enclosed cold-cathode triode. *Med. & Biol. Eng. & Comput.*, 32:289-294, 1994.

12) Takahashi K, Sato E, Sagae M, Oizumi T, Tamakawa Y and Yanagisawa T: Fundamental study on a long-duration flash x-ray generator with a surface-discharge triode. *Jpn. J. Appl. Phys.*, 33: 4146-4151, 1994.

13) Sato E, Sagae M, Shikoda A, Takahashi K, Oizumi T, Yamamoto M, Takabe A, Sakamaki K, Hayasi Y, Ojima H, Takayama K and Tamakawa Y: High-speed soft x-ray techniques, *SPIE*, 2869: 937-955, 1996.

14) Sato E, Hayasi Y, Tanaka E, Mori H, Kawai T, Usuki T, Sato K, Obara H, Ichimaru T, Takayama K, Ido H and Tamakawa Y: Quasi-monochromatic radiography using a high-intensity quasi-x-ray laser generator. *SPIE*, 4682:538-548, 2002.

15) Sato E, Hayasi Y, Germer R, Tanaka E, Mori H, Kawai T, Obara H, Ichimaru T, Takayama K and Ido H: Intense characteristic x-ray irradiation from weakly ionized linear plasma and applications. *Jpn. J. Med. Imag. Inform. Sci.*, 20:148-155. 2003.

16) Sato E, Hayasi Y, Germer R, Tanaka E, Mori H, Kawai T, Obara H, Ichimaru T, Takayama K and Ido H: Irradiation of intense characteristic x-rays from weakly ionized linear molybdenum plasma. *Jpn. J. Med. Phys.*, 23:123-131, 2003.

17) Sato E, Hayasi Y, Germer R, Tanaka E, Mori H, Kawai T, Ichimaru T, Takayama K and Ido H: Quasi-monochromatic flash x-ray generator utilizing weakly ionized linear copper plasma. *Rev. Sci. Instrum.*, 74:5236-5240, 2003.

18) Sato E, Hayasi Y, Germer R, Tanaka E, Mori H, Kawai T, Ichimaru T, Sato S, Takayama K and Ido H: Sharp characteristic x-ray irradiation from weakly ionized linear plasma. *J. Electron Spectrosc. Related Phenom.*, 137-140:713-720, 2004.

19) Sato E, Germer R, Hayasi Y, Murakami K, Koorikawa Y, Tanaka E, Mori H, Kawai T, Ichimaru T, Obata F, Takahashi K, Sato S, Takayama K and Ido H: Weakly ionized cerium plasma radiography. *SPIE*, 5210:12-21, 2003.

20) Sato E, Tanaka E, Mori H, Kawai T, Ichimaru T, Sato S, Takayama K and Ido H: Demonstration of enhanced K-edge angiography using a cerium target x-ray generator. *Med. Phys.*, 31: 3017-3022, 2004.

21) Sato E, Sato K and Tamakawa Y: Film-less computed radiography system for high-speed Imaging. *Ann. Rep. Iwate Med. Univ. Sch. Lib. Arts and Sci.*, 35:13-23, 2000.

セリウムX線装置と酸化セリウムフィルターを利用したコーンビームKエッジ造影
―― 微小血管の観察 ――

市丸俊夫[*1] 山寺 亮[*1] 佐藤英一[*2]
田中越郎[*3] 盛 英三[*4] 河合敏明[*5]
佐藤成大[*6] 高山和喜[*7]

(2004年10月30日受付, 2005年1月13日受理)

要旨：セリウム対陰極から発生するK系列特性X線はヨウ素系造影剤に効率良く吸収されるので，コーンビームによるKエッジ造影に有用である。X線装置はメインコントローラー，そして高電圧回路とX線管のユニットなどからなる。X線管はガラス封じ込み二極管で，セリウム対陰極と0.5 mm厚のベリリウム窓を有する。管電圧と電流の最大値はそれぞれ65 kVと0.4 mAで，実効焦点サイズは1.3×0.9 mmであった。セリウムのK系列特性X線は酸化セリウムのフィルターを用いて制動X線を吸収することにより得られ，X線強度は線源から1.0 mの位置で，管電圧60 kV，そして管電流0.4 mAの条件下で，0.5 μC/kg•sであった。血管には直径15 μmのヨウ素プラスチック微小球が充填され，デジタル撮影装置（CR）で造影された。動物ファントムの造影では，100 μm程度の血管が高コントラストで観察できた。

キーワード：X線発生装置，セリウムターゲット，準単色X線，特性X線，Kエッジ造影

*1弘前大学医学部保健学科放射線技術科学専攻
〒036-8565 青森県弘前市本町66番地1
*2岩手医科大学教養部物理学科
〒020-0015 岩手県盛岡市本町通3-16-1
*3東京農業大学応用生物科学部栄養科学科
〒020-0015 東京都世田谷区桜ヶ丘1-1-1
*4国立循環器センター研究所心臓生理部
〒565-8565 大阪府吹田市藤白台5-7-1
*5浜松ホトニクス電子管事業部
〒438-0193 静岡県磐田郡豊岡村下神増314-5
*6岩手医科大学医学部細菌学講座
〒020-0015 岩手県盛岡市内丸19-1
*7東北大学流体力学研究所
〒980-8577 宮城県仙台市青葉区片平2-1-1

Cardiovascular Drugs and Therapy 19 33–40 2005

BASIC PHARMACOLOGY

Erythropoietin Just Before Reperfusion Reduces Both Lethal Arrhythmias and Infarct Size via the Phosphatidylinositol-3 Kinase-Dependent Pathway in Canine Hearts

Akio Hirata[1], Tetsuo Minamino[1], Hiroshi Asanuma[1], Shoji Sanada[1], Masashi Fujita[1], Osamu Tsukamoto[1], Masakatsu Wakeno[2], Masafumi Myoishi[2], Ken-ichiro Okada[1], Hidekazu Koyama[1], Kazuo Komamura[3], Seiji Takashima[1], Yoshiro Shinozaki[4], Hidezo Mori[3], Hitonobu Tomoike[3], Masatsugu Hori[1], and Masafumi Kitakaze[3]

[1]*Department of Internal Medicine and Therapeutics, Osaka University Graduate School of Medicine, Suita, Osaka, Japan;* [2]*Department of Bioregulatory Medicine, Osaka University Graduate School of Medicine, Suita, Osaka, Japan;* [3]*Cardiovascular Division of Internal Medicine, National Cardiovascular Center, Suita, Osaka, Japan;* [4]*Department of Physiological Science, Tokai University School of Medicine, Isehara, Kanagawa, Japan*

Summary. **Although recent studies suggest that erythropoietin (EPO) may reduce multiple features of the myocardial ischemia/reperfusion injury, the cellular mechanisms and the clinical implications of EPO-induced cardioprotection are still unclear. Thus, in this study, we clarified dose-dependent effects of EPO administered just before reperfusion on infarct size and the incidence of ventricular fibrillation and evaluated the involvement of the phosphatidylinositol-3 (PI3) kinase in the *in vivo* canine model. The canine left anterior descending coronary artery was occluded for 90 min followed by 6 h of reperfusion. A single intravenous administration of EPO just before reperfusion significantly reduced infarct size (high dose (1,000 IU/kg): 7.7 ± 1.6%, low dose (100 IU/kg): 22.1 ± 2.4%, control: 40.0 ± 3.6%) in a dose-dependent manner. Furthermore, the high, but not low, dose of EPO administered as a single injection significantly reduced the incidence of ventricular fibrillation during reperfusion (high dose: 0%, low dose: 40.0%, control: 50.0%). An intracoronary administration of a PI3 kinase inhibitor, wortmannin, blunted the infarct size-limiting and anti-arrhythmic effects of EPO. Low and high doses of EPO equally induced Akt phosphorylation and decreased the equivalent number of TUNEL-positive cells in the ischemic myocardium of dogs. These effects of EPO were abolished by the treatment with wortmannin. In conclusion, EPO administered just before reperfusion reduced infarct size and the incidence of ventricular fibrillation via the PI3 kinase-dependent pathway in canine hearts. EPO administration can be a realistic strategy for the treatment of acute myocardial infarction.**

Key Words. **erythropoietin, myocardial infarction, ventricular arrhythmia, phosphatidylinositol-3 kinase, ischemia-reperfusion injury, apoptosis**

Introduction

Recent studies have extended the traditional role of erythropoietin (EPO) from a mediator of erythroid maturation to one that provides protection against apoptotic cell death [1,2]. Recombinant human EPO (rhEPO) has been shown to exert marked protective effects against ischemia/reperfusion injury in rats and rabbits when rhEPO is administered at different time points [3–8]. Indeed, rhEPO reduced myocardial infarct size, enhanced recovery of left ventricular developed pressure, reduced the number of apoptotic cells, and induced the phosphorylation of Akt [3–8]. In these studies, high (1,000–5,000 IU/kg) doses of rhEPO, nearly 10 times higher than that used in anemic patients with chronic renal failure [9], have been applied. Recently, it was reported that phosphatidylinositol-3 (PI3) kinase

Address for correspondence: Tetsuo Minamino, MD, PhD, Department of Internal Medicine and Therapeutics, Osaka University Graduate School of Medicine, 2-2 Yamadaoka, Suita, Osaka 565-0871, Japan, Tel.: 81-6-6879-3635; Fax: 81-6-6879-3473; E-mail: minamino@medone.med.osaka-u.ac.jp

activity is required for rhEPO to recover contractile dysfunction and to block apoptosis induced by myocardial ischemia-reperfusion in isolated hearts (*ex vivo*) [10]. However, it is not determined whether rhEPO just before reperfusion reduces infarct size via PI3 kinase-dependent pathway in the *in vivo* model.

In addition to myocardial cell death, myocardial ischemia-reperfusion triggers lethal arrhythmias [11]. It is believed that at least half of the deaths due to coronary artery disease are caused by a lethal arrhythmia [12]. Although high doses of rhEPO exert cardioprotective effects against ischemia/reperfusion injury in small animals [3–8], its effects on lethal arrhythmias remain unknown. If rhEPO reduces the incidence of ventricular fibrillation (VF) in the clinical setting, there would be additional advantage to use this drug in the realistic situation of acute myocardial infarction. Thus, in the present study, we examined dose-dependent effects of rhEPO administered just before reperfusion on myocardial infarct size and the incidence of VF in the *in vivo* canine model. We also evaluated whether any such effects were mediated via the PI3 kinase pathway.

Materials and Methods

Materials

Wortmannin was obtained from Sigma (St. Louis, MO) and Phospho-Akt and Akt antibodies were obtained from Cell Signaling Technologies (Beverly, MA). RhEPO was provided by Chugai Pharmaceutical Co., Ltd (Tokyo, Japan).

Instrumentation

Forty-eight beagle dogs (Kitayama Labes, Yoshiki Farm, Gifu, Japan) weighing 8 to 12 kg were anesthetized by an intravenous injection of sodium pentobarbital (30 mg/kg), intubated, and ventilated with room air mixed with oxygen (100% O_2 at flow rate of 1.0 to 1.5 L/min). Thoracotomy was done at the left fifth intercostal space, and the heart was suspended by a pericardial cradle. After intravenous administration of heparin (500 U/kg), the left anterior descending coronary artery (LAD) was cannulated for perfusion with blood from the left carotid artery through an extracorporeal bypass tube. Coronary blood flow was measured with an electromagnetic flow probe attached to the bypass tube. We can selectively infuse drugs into LAD-perfused areas through this bypass tube. The left atrium was catheterized for microsphere injection to measure myocardial collateral blood flow during ischemia. Hydration was maintained by a slow normal saline infusion. The femoral artery was also cannulated to measure the mean systemic blood pressure (SBP). Both SBP and heart rate (HR) were monitored continuously during the study. All procedures were performed in conformity with the *Guide for the Care and Use of Laboratory Animals* (NIH Publication No. 85–23, 1996 revision), and were approved by the Osaka University Committee for Laboratory Animal Use.

Experimental protocols

Protocol 1. Long-term effects of rhEPO on hematometric parameters in dogs. To test the long-term effects of rhEPO on hematometric parameters, 100 IU/kg ($n = 5$) or 1,000 IU/kg ($n = 5$) of rhEPO was intravenously administered as a single injection. Blood was collected under pentobarbital (15 mg/kg) anesthesia before and 7, 14 days after rhEPO treatment. Hematometric parameters including hematocrit, white blood cell, and platelet counts were measured.

Protocol 2; Measurement of infarct size, coronary blood flow and myocardial collateral blood flow. After hemodynamic stabilization, we administered a low (100 IU/kg), or high (1,000 IU/kg) dose of rhEPO, or saline 10 min prior to reperfusion (n = 8–12 each) as a single intravenous injection (Fig. 1). To clarify whether rhEPO reduces myocardial infarct size through a PI3 kinase-dependent pathway, a PI3 kinase inhibitor, wortmannin, was selectively administered into the LAD (1.5 μg/kg/min) for 60 min after the onset of reperfusion. We have previously confirmed that the dose of wortmannin employed in this study is appropriate for blocking the phosphorylation of Akt in myocardium [13]. We measured infarct size and regional myocardial collateral blood flow during 90 min of ischemia as described previously [14]. In brief, infarct size was evaluated at the end of the protocol by Evans blue/TTC staining, while collateral blood flow was assessed by the non-radioactive microsphere method [14]. Coronary blood flow was monitored continuously during the study. To ensure that all of the animals included in the data analysis were healthy and were exposed to a similar extent of ischemia, the exclusion criteria reported previously for excessive myocardial collateral blood flow (>15 mL/100 g/min) and lethal arrhythmia (more than two consecutive attempts required to convert VF with low-energy DC pulses applied directly to the heart) were adopted [14].

Effects of rhEPO on VF during reperfusion period

In Protocol 2, we also evaluated the incidence of VF during the 6 h reperfusion period (Fig. 1). Since myocardial collateral blood flow during ischemia exhibited a negative correlation with the incidence of VF [15,16], the dogs with excessive collateral blood flow (>15 mL/100 g/min) were excluded from VF analysis.

Phosphorylation of Akt

We used 12 dogs for western blot in the control, low EPO, high EPO, and high EPO + WTMN groups ($n = 3$ each) in Protocol 2 (Fig. 1). After 90 min of ischemia followed by 6 h of reperfusion, hearts were excised and

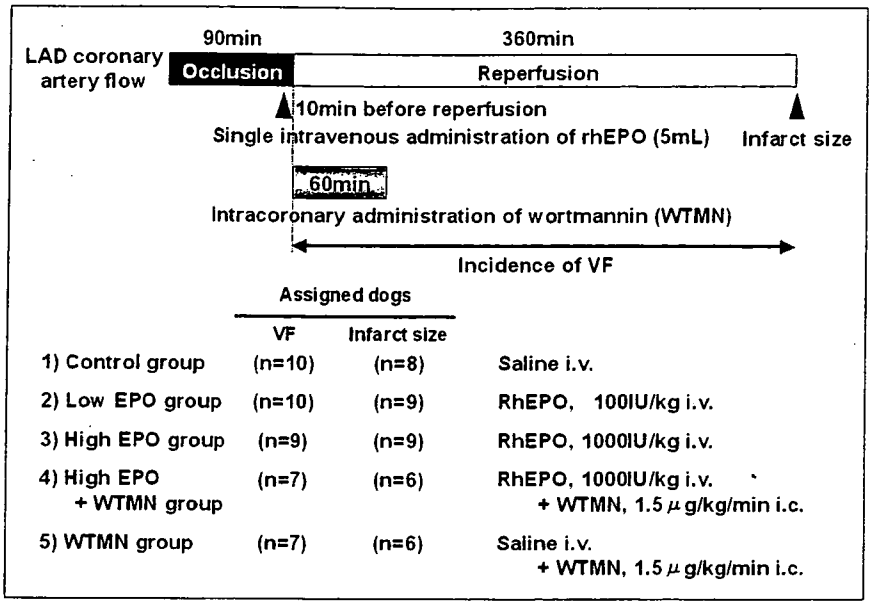

Fig. 1. Experimental protocol for infarct size and VF.

the myocardial tissue in the ischemic zone was quickly placed into liquid nitrogen and stored at −80°C. Phosphorylation of Akt and total content of Akt were evaluated as reported previously [13]. The immunoreactive bands were quantified by densitometry (Molecular Dynamics).

Terminal deoxynucleotidyl transferase-mediated dUTP nick-end labeling (TUNEL)

In Protocol 2, the myocardial tissue samples were taken from the ischemic zone of dogs in the control, low EPO, high EPO, and high EPO + WTMN groups ($n = 3$ each). These were fixed in 10% buffered formalin, embedded in paraffin, and serially sectioned in the frontal plane at 5-μm thickness. Analysis by TUNEL method was performed according to the protocol supplied with the in situ apoptosis detection kit, the Apop Tag Peroxidase *In Situ* Apoptosis Detection Kit (CHEMICON International, USA). TUNEL-positive cell nuclei and total cell nuclei stained metylgreen were counted in 10–15 random high-power fields (×400), and the percentage of TUNEL-positive cell nuclei to total cell nuclei ($n =$ 1,000) were then calculated.

Statistical analysis

Statistical analysis was performed by one-way factional analysis of variance (ANOVA) with modified Bonferroni's post hoc test when the data were compared among groups. Time courses of the changes were compared by repeated measures ANOVA. The incidence of VF was compared using the χ^2-test and Fisher's exact probability test. Results were expressed as the mean ± SEM, with $p < 0.05$ considered significant.

Results

The long-term effects of rhEPO on hematometric parameters

The single administration of either 100 IU/kg or 1,000 IU/kg of rhEPO did not change any hematometric parameters including hematocrit, white blood cells, and platelet counts 7 or 14 days after rhEPO treatment (Table 1).

Table 1. *Long-term effects of rhEPO on hematometric parameters in dogs*

	EPO 100 IU/kg			EPO 1000 IU/kg		
Parameters	Day 0	Day 7	Day 14	Day 0	Day 7	Day 14
Ht (%)	50.1 ± 0.8	51.1 ± 0.9	51.3 ± 1.0	51.5 ± 1.3	52.0 ± 1.0	53.1 ± 0.7
WBC ($10^3/\mu$L)	11.7 ± 1.3	12.1 ± 0.7	11.4 ± 0.6	11.5 ± 1.3	11.7 ± 0.7	12.0 ± 1.0
Platelet ($10^4/mm^3$)	33.7 ± 2.0	33.7 ± 1.8	33.3 ± 1.7	33.2 ± 1.9	34.0 ± 2.4	36.4 ± 3.4

Data are presented as Mean ± SEM. $n = 5$.

Abbreviations: rhEPO = recombinant human erythropoietin, Ht = hematocrit, WBC = white blood cell.

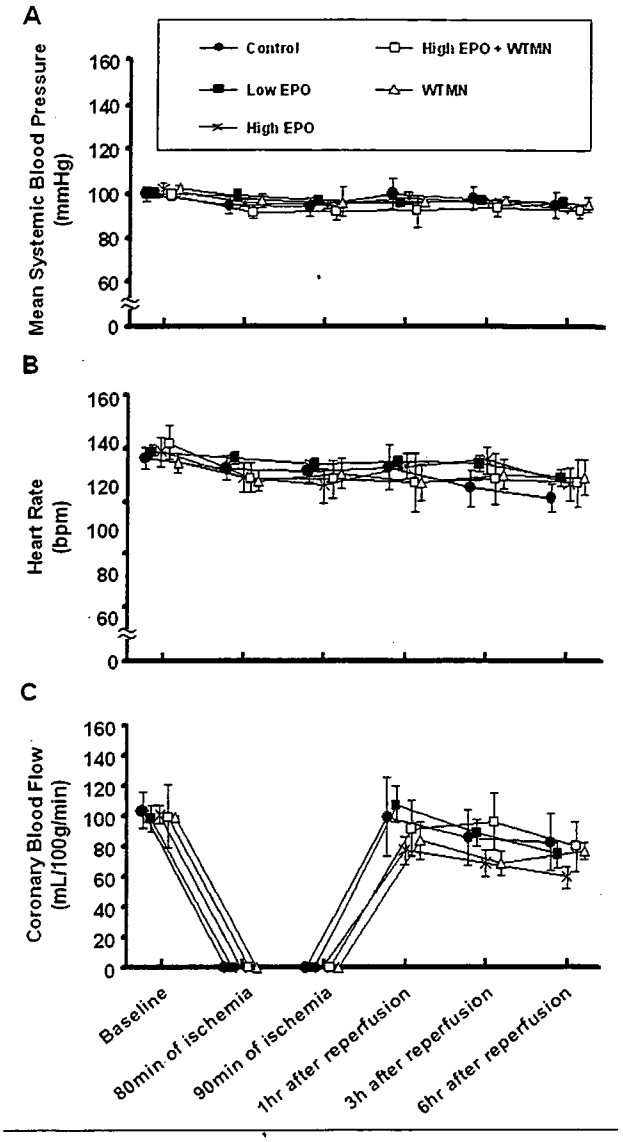

Fig. 2. The changes in mean systemic blood pressure, heart rate and coronary blood flow during the experiment in groups tested.

Effects of rhEPO on infarct size and VF during the reperfusion period

Since 5 of 48 dogs were excluded from analysis because of excessive collateral blood flow (>15 mL/100 g/min) (control: 1, low EPO: 2, high EPO: 1, high EPO + WTMN: 0, WTMN: 1), 43 dogs were evaluated for VF analysis. Among these 43 dogs, we excluded 5 dogs (control: 2, low EPO: 1, high EPO: 0, high EPO + WTMN: 1, WTMN: 1) that matched the exclusion criteria of lethal arrhythmia from infarct size analysis.

Throughout the study, neither SBP (Fig. 2A), nor HR (Fig. 2B), nor coronary blood flow (Fig. 2C) differed among the 5 groups. The area at risk (Fig. 3A) and myocardial collateral blood flow in the LAD region during myocardial ischemia (Fig. 3B) were also comparable in the groups tested.

Table 2. Effects of rhEPO on the incidence of VF during reperfusion periods

Group	Incidence of VF	
Control	50.0%	(5/10)
Low EPO	40.0%	(4/10)
High EPO	0%*	(0/9)
High EPO + WTMN	42.9%	(3/7)
WTMN	42.9%	(3/7)

*$p < 0.05$ vs. control group.

Abbreviations: VF = ventricular fibrillation, rhEPO = recombinant human erythropoietin, WTMN = wortmannin.

Figure 4 shows infarct size in the groups tested. A low or high dose of rhEPO significantly ($p < 0.05$) reduced the infarct size compared with that in the control group. Furthermore, a high dose of rhEPO reduced infarct size more than a low dose of rhEPO did. The intracoronary administration of wortmannin for 60 min after the onset of reperfusion abrogated the infarct-limiting effect of rhEPO, although wortmannin alone did not affect infarct size.

The high, but not low, dose of rhEPO significantly ($p < 0.05$) reduced the incidence of VF during the 6 h reperfusion period compared with the control. The anti-arrhythmic effects of rhEPO were abolished by wortmannin (Table 2).

Effects of rhEPO on Akt phosphorylation

After 90 min of ischemia followed by 6 h of reperfusion, the ratio of phosphorylated Akt to total Akt in the low and high EPO groups significantly ($p < 0.05$) increased compared with that in the control group. The increase in this ratio was completely abolished by the treatment with wortmannin (Fig. 5).

Effects of rhEPO on apoptosis

The ratio of TUNEL positive cells to total cells in the low and high EPO groups decreased compared with that in the control group. The reduction of TUNEL-positive cells by rhEPO was completely abolished by the treatment with wortmannin (Fig. 6).

Discussion

In this study, we demonstrated that a single intravenous administration of rhEPO just before reperfusion limited not only infarct size but also the incidence of VF. Moreover, our data suggest that the infarct size-limiting and anti-arrhythmic effects of rhEPO were through the PI3 kinase-dependent pathways in the *in vivo* canine hearts.

Important considerations towards clinical application of rhEPO are the timing and dose of its administration. The previous studies reported that rhEPO administered at the onset of reperfusion [7,8] as well

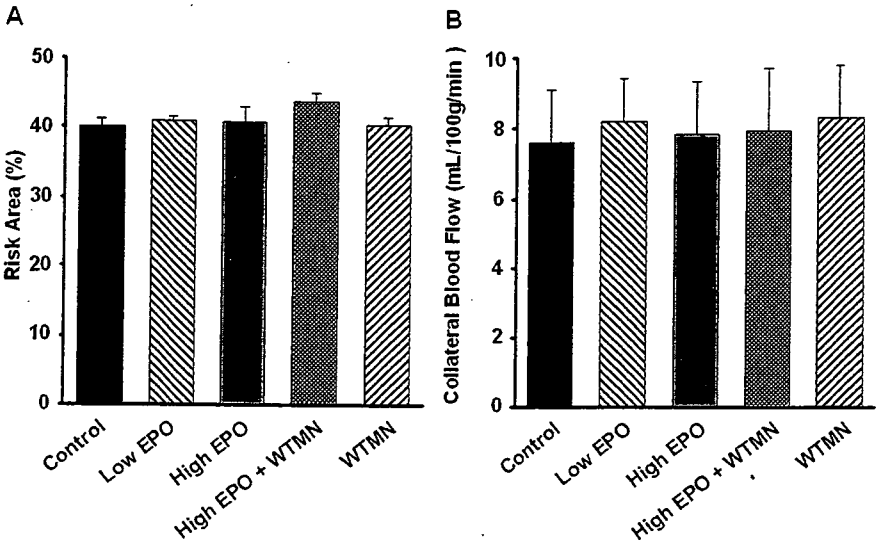

Fig. 3. Area at risk and myocardial collateral blood flow during ischemia in groups tested.

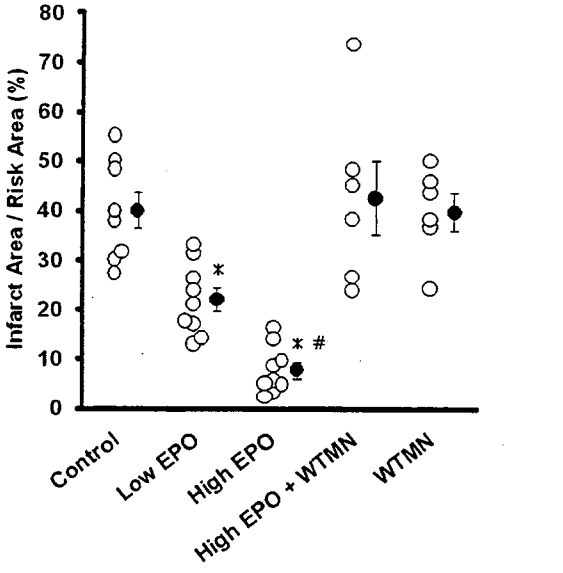

*Fig. 4. Infarct size in groups tested. *p < 0.05 vs. control group. #p < 0.05 vs. low EPO group. Open circles show the infarct size in each individual.*

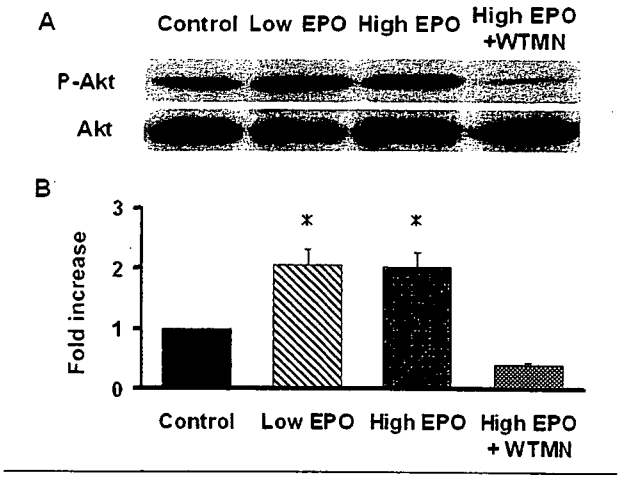

*Fig. 5. Phosphorylation of Akt in canine hearts. (A) Representative Western blot for phosphorylated and total Akt. (B) Densitometry graphs indicating fold expression over control for Akt. n = 3 each. *p < 0.05 vs. control group.*

as ischemia [7,8] reduces infarct size in rabbit and rat hearts. Consistent with these reports, we confirmed that rhEPO administered 10 min before reperfusion reduced myocardial infarct size in dogs. Our findings support the idea that in humans the adjunctive therapy with rhEPO treatment during coronary intervention would reduce myocardial infarct size.

The doses of rhEPO (1,000–5,000 IU/kg) administered in previous experimental studies [3–8] were nearly 10 times higher than those clinically used in anemic patients with chronic renal failure [9]. In the present study, we demonstrated that both 100 IU/kg and 1,000 IU/kg of rhEPO as a single administration significantly reduced myocardial infarct size, although a high dose of rhEPO significantly reduced infarct size more than a low dose of rhEPO did. This finding suggests that the clinically relevant dose of rhEPO used in patients with chronic renal failure can reduce myocardial infarct size. In the previous clinical studies, a high dose (33,000 IU once daily for the first 3 days) of intravenously administered rhEPO was well tolerated in patients with stroke and improved clinical outcome at 1 month [17]. On the other hand, a high dose (40,000–60,000 IU per week) of subcutaneously administered rhEPO, while not as a single injection,

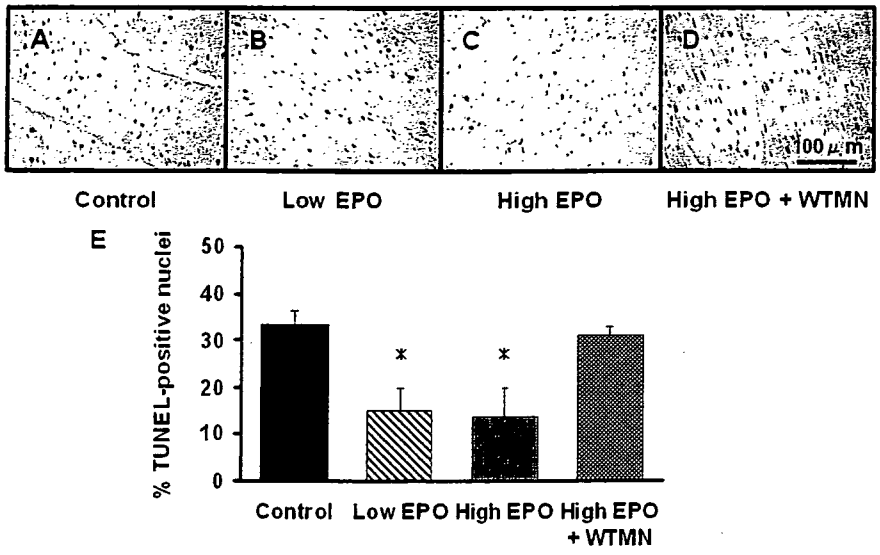

*Fig. 6. TUNEL staining in canine hearts after 90 min ischemia followed by 6 h of reperfusion. Representative examples of TUNEL-staining from canine hearts in the control (A), low EPO (B), high EPO (C), and high EPO + WTMN groups (D). (E) Quantitative data of the percentage of TUNEL-positive nuclei to total cell nuclei. *p < 0.05 vs. control group.*

increased the incidence of thrombotic events such as deep venous thrombosis or pulmonary embolisms in patients with breast cancer [18]. Furthermore, there are some reports that rhEPO increases the number of platelets in normal rats [19] and chronically hemodialyzed patients [20]. In the present study, we didn't find that either low or high dose of rhEPO, as a single injection, changed hematometric parameters. Although these findings suggest that a single administration of 1,000 IU/kg of rhEPO, that induced marked reduction of myocardial infarct size, could be used safely, we must be careful for the use of a high dose of rhEPO for the treatment of myocardial infarction.

Previous reports have shown that both phosphorylation of Akt and inhibition of apoptosis are associated with infarct size-limiting effects due to rhEPO [4,6–8]. Recently, it was reported that PI3 kinase activity is required for rhEPO to recover contractile dysfunction and to block apoptosis induced by myocardial ischemia-reperfusion in isolated hearts (*ex vivo*) [10]. Although the recovery of contractile function could be related to the reduction of infarct size, no evidence was presented that rhEPO reduced infarct size via the PI3 kinase-dependent pathway. In the present study we have demonstrated that the infarct size-limiting effect of rhEPO was blunted by the intracoronary administration of wortmannin in dogs. This is the first evidence showing that the infarct size-limiting effect of rhEPO is dependent on the PI3 kinase pathway in *in vivo* hearts.

In the present study, low and high doses of rhEPO equally increased phosphorylation of Akt and decreased equivalent number of TUNEL-positive cells in the ischemic myocardium of dogs. Either Akt phosphorylation or a decrease in the number of TUNEL-positive cells was prevented by the PI3 kinase inhibitor, wortmannin. This finding suggests that rhEPO prevents apoptotic cell death through PI3 kinase/Akt-dependent pathway in canine hearts. However, since the TUNEL method also detects single strand breaks occurring in the course of necrotic cell death [21], it is likely that rhEPO attenuates apoptotic and necrotic cell death. Indeed, if rhEPO only inhibits the apoptotic cell death, it may be difficult to explain the marked reduction of infarct size by rhEPO. Interestingly, the previous studies reported that the PI3 kinase activates not only Akt but also protein kinase C or mitogen-activated protein kinase in ischemia/reperfusion models [22–24], either of which mediates the cellular protection against necrotic process [25,26]. Furthermore, recent reports suggest that rhEPO can inhibit the release of free radicals from neutrophils [27] and act as a radical scavenger [28], both of which may reduce cardiac cell death after ischemia/reperfusion. Although further investigation will be needed, these characteristics of rhEPO may contribute to the reduction of necrotic as well as apoptotic cell death in ischemia/reperfused myocardium. In addition, since wortmannin inhibits not only PI3 kinase but also PI4 kinase and PI kinase related protein kinase, there is a limitation in using wortmannin as a specific inhibitor of PI3 kinase [29].

In clinical settings, ventricular arrhythmias are often observed in patients following reperfusion therapy and they can be life-threatening [30]. Importantly, the present study demonstrated that a high, but not a low dose of rhEPO prevented VF during reperfusion via the PI3 kinase-dependent pathway. Since low and high doses of rhEPO equally increased phosphorylation of Akt, it is unlikely that Akt is responsible for

the rhEPO-induced anti-arrhythmic effect. There are several possible mechanisms by which rhEPO exerts anti-arrhythmic effects via the PI3 kinase-dependent, but Akt-independent, pathway. First, under conditions of reperfusion, production of inositol-1,4,5-trisphospate (IP3) increases when phospholipase C (PLC) is activated through α-adrenoreceptors on the myocardial cell membrane [11]. This increase in IP3 activates IP3 receptors on the sarcoplasmic reticulum causing the release of Ca^{2+}. The increases in the intracellular Ca^{2+} levels caused by IP3 have been reported to initiate slow Ca^{2+} oscillations, which underlies the delayed afterdepolarizations that trigger many arrhythmias including VF [11,31]. PLC hydrolyzes phosphatidylinositol-4,5-bisphospate (PIP2) to produce IP3. Since PI3 kinase and PLC can act upon the common substrate, PIP2 [32], rhEPO may prevent lethal arrhythmia by activating the PI3 kinase pathway that results in the decrease in PIP2 levels, which will lead to prevent Ca^{2+} overload by IP3. Second, since oxygen-derived free radicals are involved in the generation of reperfusion arrhythmia [30,33,34], rhEPO may decrease reperfusion arrhythmia through the prevention of free radicals release from neutrophils or acting as a radical scavenger [27,28]. Finally, we need to consider that rhEPO exerts anti-arrhythmic effects by the reduction of myocardial infarct size.

In conclusion, our findings, when translated into clinical practice, may support the use of rhEPO as a cardioprotective agent in the treatment of patients with myocardial infarction.

Acknowledgments

We thank Yuko Okuda, Yoko Nagamachi, Nobuko Kawasaki and Tomi Fukushima for their technical assistance.

References

1. Siren AL, Fratelli M, Brines M, et al. Erythropoietin prevents neuronal apoptosis after cerebral ischemia and metabolic stress. *Proc Natl Acad Sci USA* 2001;98:4044–4049.
2. van der Meer P, Voors AA, Lipsic E, van Gilst WH, van Veldhuisen DJ. Erythropoietin in cardiovascular diseases. *Eur Heart J* 2004;25:285–291.
3. Calvillo L, Latini R, Kajstura J, et al. Recombinant human erythropoietin protects the myocardium from ischemia-reperfusion injury and promotes beneficial remodeling. *Proc Natl Acad Sci USA* 2003;100:4802–4806.
4. Tramontano AF, Muniyappa R, Black AD, et al. Erythropoietin protects cardiac myocytes from hypoxia-induced apoptosis through an Akt-dependent pathway. *Biochem Biophys Res Commun* 2003;308:990–994.
5. Moon C, Krawczyk M, Ahn D, et al. Erythropoietin reduces myocardial infarction and left ventricular functional decline after coronary artery ligation in rats. *Proc Natl Acad Sci USA* 2003;100:11612–11617.
6. Parsa CJ, Matsumoto A, Kim J, et al. A novel protective effect of erythropoietin in the infarcted heart. *J Clin Invest* 2003;112:999–1007.
7. Parsa CJ, Kim J, Riel RU, et al. Cardioprotective effects of erythropoietin in the reperfused ischemic heart: A potential role for cardiac fibroblasts. *J Biol Chem* 2004;279:20655–20662.
8. Lipsic E, van der Meer P, Henning RH, et al. Timing of erythropoietin treatment for cardioprotection in ischemia/reperfusion. *J Cardiovasc Pharmacol* 2004;44:473–479.
9. NKF-DOQI clinical practice guidelines for the treatment of anemia of chronic renal failure. National Kidney Foundation-Dialysis Outcomes Quality Initiative. *Am J Kidney Dis* 1997;30:S192–S240.
10. Cai Z, Semenza GL. Phosphatidylinositol-3-kinase signaling is required for erythropoietin-mediated acute protection against myocardial ischemia/reperfusion injury. *Circulation* 2004;109:2050–2053.
11. Woodcock EA, Matkovich SJ, Binah O. Ins(1,4,5)P3 and cardiac dysfunction. *Cardiovasc Res* 1998;40:251–256.
12. Billman GE, Hallaq H, Leaf A. Prevention of ischemia-induced ventricular fibrillation by omega 3 fatty acids. *Proc Natl Acad Sci USA* 1994;91:4427–4430.
13. Ogita H, Node K, Asanuma H, et al. Raloxifene improves coronary perfusion, cardiac contractility, and myocardial metabolism in the ischemic heart: Role of phosphatidylinositol 3-kinase/Akt pathway. *J Cardiovasc Pharmacol* 2004;43:821–829.
14. Ogita H, Node K, Asanuma H, et al. Amelioration of ischemia- and reperfusion-induced myocardial injury by the selective estrogen receptor modulator, raloxifene, in the canine heart. *J Am Coll Cardiol* 2002;40:998–1005.
15. Hale SL, Lange R, Alker KJ, Kloner RA. Correlates of reperfusion ventricular fibrillation in dogs. *Am J Cardiol* 1984;53:1397–1400.
16. Bolli R, Patel B. Factors that determine the occurrence of reperfusion arrhythmias. *Am Heart J* 1988;115:20–29.
17. Ehrenreich H, Hasselblatt M, Dembowski C, et al. Erythropoietin therapy for acute stroke is both safe and beneficial. *Mol Med* 2002;8:495–505.
18. Rosenzweig MQ, Bender CM, Lucke JP, Yasko JM, Brufsky AM. The decision to prematurely terminate a trial of R-HuEPO due to thrombotic events. *J Pain Symptom Manage* 2004;27:185–190.
19. Berridge MV, Fraser JK, Carter JM, Lin FK. Effects of recombinant human erythropoietin on megakaryocytes and on platelet production in the rat. *Blood* 1988;72:970–977.
20. Tang WW, Stead RA, Goodkin DA. Effects of Epoetin alfa on hemostasis in chronic renal failure. *Am J Nephrol* 1998;18:263–273.
21. Ohno M, Takemura G, Ohno A, et al. "Apoptotic" myocytes in infarct area in rabbit hearts may be oncotic myocytes with DNA fragmentation: Analysis by immunogold electron microscopy combined with In situ nick end-labeling. *Circulation* 1998;98:1422–1430.
22. Mizukami Y, Hirata T, Yoshida K. Nuclear translocation of PKC zeta during ischemia and its inhibition by wortmannin, an inhibitor of phosphatidylinositol 3-kinase. *FEBS Lett* 1997;401:247–251.
23. Mizukami Y, Kobayashi S, Uberall F, Hellbert K, Kobayashi N, Yoshida K. Nuclear mitogen-activated protein kinase activation by protein kinase czeta during reoxygenation after ischemic hypoxia. *J Biol Chem* 2000;275:19921–19927.

24. Takeda H, Matozaki T, Takada T, et al. PI 3-kinase gamma and protein kinase C-zeta mediate RAS-independent activation of MAP kinase by a Gi protein-coupled receptor. *Embo J* 1999;18:386–395.
25. Ping P, Zhang J, Zheng YT, et al. Demonstration of selective protein kinase C-dependent activation of Src and Lck tyrosine kinases during ischemic preconditioning in conscious rabbits. *Circ Res* 1999;85:542–550.
26. Sanada S, Kitakaze M, Papst PJ, et al. Role of phasic dynamism of p38 mitogen-activated protein kinase activation in ischemic preconditioning of the canine heart. *Circ Res* 2001;88:175–180.
27. Kristal B, Shurtz-Swirski R, Shasha SM, et al. Interaction between erythropoietin and peripheral polymorphonuclear leukocytes in hemodialysis patients. *Nephron* 1999;81:406–413.
28. Chattopadhyay A, Choudhury TD, Bandyopadhyay D, Datta AG. Protective effect of erythropoietin on the oxidative damage of erythrocyte membrane by hydroxyl radical. *Biochem Pharmacol* 2000;59:419–425.
29. Stein RC. Prospects for phosphoinositide 3-kinase inhibition as a cancer treatment. *Endocr Relat Cancer* 2001;8:237–248.
30. Jeroudi MO, Hartley CJ, Bolli R. Myocardial reperfusion injury: Role of oxygen radicals and potential therapy with antioxidants. *Am J Cardiol* 1994;73:2B–7B.
31. Van Wagoner DR, Bond M. Reperfusion arrhythmias: New insights into the role of the Na(+)/Ca(2+) exchanger. *J Mol Cell Cardiol* 2001;33:2071–2074.
32. Marshall AJ, Niiro H, Yun TJ, Clark EA. Regulation of B-cell activation and differentiation by the phosphatidylinositol 3-kinase and phospholipase Cgamma pathway. *Immunol Rev* 2000;176:30–46.
33. Lee YM, Hsiao G, Chen HR, Chen YC, Sheu JR, Yen MH. Magnolol reduces myocardial ischemia/reperfusion injury via neutrophil inhibition in rats. *Eur J Pharmacol* 2001;422:159–167.
34. Hansen PR. Myocardial reperfusion injury: Experimental evidence and clinical relevance. *Eur Heart J* 1995;16:734–740.

ELSEVIER

Cardiovascular Research 65 (2005) 334–344

Cardiovascular Research

www.elsevier.com/locate/cardiores

Purified cardiomyocytes from bone marrow mesenchymal stem cells produce stable intracardiac grafts in mice

Naoichiro Hattan[a,1], Haruko Kawaguchi[b,1], Kiyoshi Ando[c], Eriko Kuwabara[a], Jun Fujita[d], Mitsushige Murata[d], Makoto Suematsu[b], Hidezo Mori[a], Keiichi Fukuda[d,*]

[a]*Department of Physiology, Tokai University School of Medicine, Japan*
[b]*Department of Biochemistry and Integrative Medical Biology, Keio University School of Medicine, Tokyo, Japan*
[c]*Department of Hematology and Oncology, Tokai University School of Medicine, Japan*
[d]*Department of Medicine, Division of Cardiology, Keio University School of Medicine, 35 Shinanomachi, Shinjuku-ku, Tokyo 160-8582, Japan*

Received 16 April 2004; received in revised form 4 October 2004; accepted 5 October 2004
Available online 28 October 2004
Time for primary review 21 days

Abstract

Objective: We have previously isolated cardiomyogenic cells from murine bone marrow (CMG cells). Regenerated cardiomyocytes are important candidates for cell transplantation, but as they are stem cell derived, they can be contaminated with various cell types, thereby requiring characterization and purification. Our objectives were to increase the efficiency of cell transplantation and to protect the recipients from possible adverse effects using an efficient and effective purification process as well as to characterize regenerated cardiomyocytes.
Methods: Noncardiomyocytes were eliminated from a mixture of stem-cell-derived cells using a fluorescence-activated cell sorter to specifically isolate CMG cells transfected with a recombinant plasmid containing enhanced green fluorescent protein (EGFP) cDNA under the control of the myosin light chain-2v (MLC-2v) promoter. Gene expression and the action potential were investigated, and purified cells were transplanted into the heart of adult mice.
Results: Six percent to 24% of transfected CMG cells expressed EGFP after differentiation was induced, and a strong EGFP-positive fraction was selected. All the sorted cells began spontaneous beating after 3 weeks. These cells expressed cardiomyocyte-specific genes such as α-skeletal actin, β-myosin heavy chain, MLC-2v, and CaV1.2 and incorporated bromodeoxyuridine for 5 days. The isolated EGFP-positive cells were expanded for 5 days and then transplanted into the left ventricle of adult mouse hearts. The transplanted cells survived for at least 3 months and were oriented in parallel to the cardiomyocytes of the recipient heart.
Conclusions: The purification and transplantation of differentiated cardiomyocytes from adult stem cells provides a viable model of tissue engineering for the treatment of heart failure.

Keywords: Cardiomyocytes; Heart failure; Transplantation; Stem cell; Bone marrow

This article is referred to in the Editorial by B. Dawn and R. Bolli (pages 293–295) in this issue.

1. Introduction

Necrotic cardiomyocytes in infarcted ventricular tissue are progressively replaced by fibroblasts leading to the formation of scar tissue and this loss of cardiomyocytes leads to regional contractile dysfunction. Transplanted fetal cardiomyocytes can survive in heart scar tissue, thereby limiting scar expansion and preventing post-infarction heart failure [1–3]. The transplantation of cultured cardiomyocytes into damaged myocardium has been proposed as a novel method

* Corresponding author. Tel.: +81 3 5363 3874; fax: +81 3 5363 3875.
E-mail address: kfukuda@sc.itc.keio.ac.jp (K. Fukuda).
[1] Naoichiro Hattan and Haruko Kawaguchi contributed equally to this paper.

0008-6363/$ - see front matter © 2004 European Society of Cardiology. Published by Elsevier B.V. All rights reserved.
doi:10.1016/j.cardiores.2004.10.004

for treating heart failure. While this is a revolutionary idea, it remains clinically unfeasible due to the difficulty in obtaining donor fetal hearts. For this reason, research has focused on the development of a cardiomyogenic cell line to treat heart failure by transplantation therapy.

Advances in regenerative medicine have enabled the generation of various cell types from embryonic stem (ES) cells or adult stem cells [4,5]. We recently reported the generation of cardiomyocytes from marrow mesenchymal stem cells in vitro (CMG cells) and demonstrated that these cells spontaneously beat, express atrial natriuretic factors, and possess a fetal ventricular cardiomyocyte-like phenotype [6]. We also reported that cardiomyocytes regenerated from marrow mesenchymal stem cells express α_{1A}, α_{1B}, α_{1D}, β_1, and β_2 adrenergic receptors and M_1 and M_2 muscarinic receptors [7]. Stimulation of the α_1 receptors with phenylephrine caused cardiomyocyte hypertrophy, and stimulation of the β receptors with isoproterenol increased the beating rate and contractility of the regenerated cardiomyocytes. These findings demonstrate the suitability of bone-marrow-derived regenerated cardiomyocytes as a candidate for use in cell transplantation therapy.

Purification of regenerated cardiomyocytes is required prior to use for cardiomyocyte transplantation. The population of cardiomyocytes in ES-cell-derived embryoid bodies is less than 10%, and the population of cardiomyocytes in 5-azacytidine-exposed CMG cells is less than 10–30%. To increase the efficiency of transplantation and protect recipients from possible adverse effects, regenerated cardiomyocytes need to be purified from the population of differentiated cell types prior to cell transplantation. Klug [8] and Muller [9] independently reported that embryonic stem-cell-derived cardiomyocytes could be purified using a cardiomyocyte-specific gene promoter–drug-resistant gene expression system. In this study, we purified bone-marrow-derived cardiomyocytes using a recombinant plasmid containing enhanced green fluorescent protein (EGFP) cDNA under the control of the myosin light chain-2v (MLC-2v) promoter. Purified cells were then transplanted into recipient mice hearts and the success of transplantation was analyzed histologically.

2. Methods

All experimental procedures and protocols were approved by the Animal Care and Use Committees of the Keio University, Japan, and the investigation conforms to the Guide for the Care and Use of Laboratory Animals published by the US National Institutes of Health (NIH Publication No. 85–23 revised 1996).

2.1. Preparation of bone marrow-derived regenerated cardiomyocytes

Murine bone-marrow-derived mesenchymal stem cells (CMG cells) were cultured in Iscove's modified Dulbecco's medium (IMDM) supplemented with 20% FBS as previously described [6,7]. The cells were exposed to 3 μmol/l of 5-azacytidine for 24 h to induce cell differentiation [6].

2.2. Construction of myosin light chain 2v-promoted EGFP plasmid

An expression vector, pMLC2v-EGFP, was constructed by cloning a 2.7-kb *Hin*dIII–*Eco*RI fragment of the rat MLC-2v promoter region [10,11] into the *Hin*dIII–*Eco*RI site of pEGFP-1 (Clontech, Palo Alto, CA), so that EGFP would be expressed under the control of MLC-2v promoter (Fig. 1a). This plasmid also contains the neomycin-resistance gene to enable selection of permanently transfected clones. MLC-2v is specifically expressed in ventricular cardiomyocytes.

2.3. Transfection of MLC2v-EGFP expression plasmid and cell selection

The MLC2v-EGFP plasmid was transfected into CMG cells by liposomal transfection. After 24 h when cells are about 20% confluent, a mixture containing 2 μg of plasmid DNA and 4 μl of LT1 TransIT Polyamine Transfection Reagent (Mirus Corporation) in OPTI-MEM (Life Technologies, Gaithersburg, MD) were added to each 35-mm culture dish. After selection with 1000 μg/ml of G418 for 4 weeks, stably transfected colonies derived from single cells were cloned and pooled. EGFP fluorescence was observed under a fluorescence microscope (Olympus TMD300, Tokyo, Japan).

2.4. Flow cytometry and cell sorting

Flow cytometry and sorting of EGFP(+) cells were performed on a FACS Vantage (Becton Dickinson, Cockeysville, MD). Cells were analyzed by light forward and side scatter and for EGFP fluorescence through a 530 nm band pass filter as they traversed the beam of an argon ion laser (488 nm, 100 mW). Nontransfected control cells were used to set the background fluorescence. Cell sorting was performed 3 days after 5-azacytidine exposure at 500 cells/s as EGFP(+) cells displaying fluorescence higher than the background level were observed at this time point.

2.5. Infection of recombinant adenovirus vectors

Replication-deficient recombinant adenovirus vector, pAdex-LacZ, was constructed by cloning LacZ cDNA into the *Swa*I site of pAdex1CAwt as previously described [12]. In this vector, *E. coli* β-galactosidase is expressed under the control of a strong, ubiquitously expressed, promoter-derived from the cytomegalovirus enhancer-chicken β-actin hybrid [13]. On day 3 after seeding, EGFP(+) cells isolated by FACS were incubated

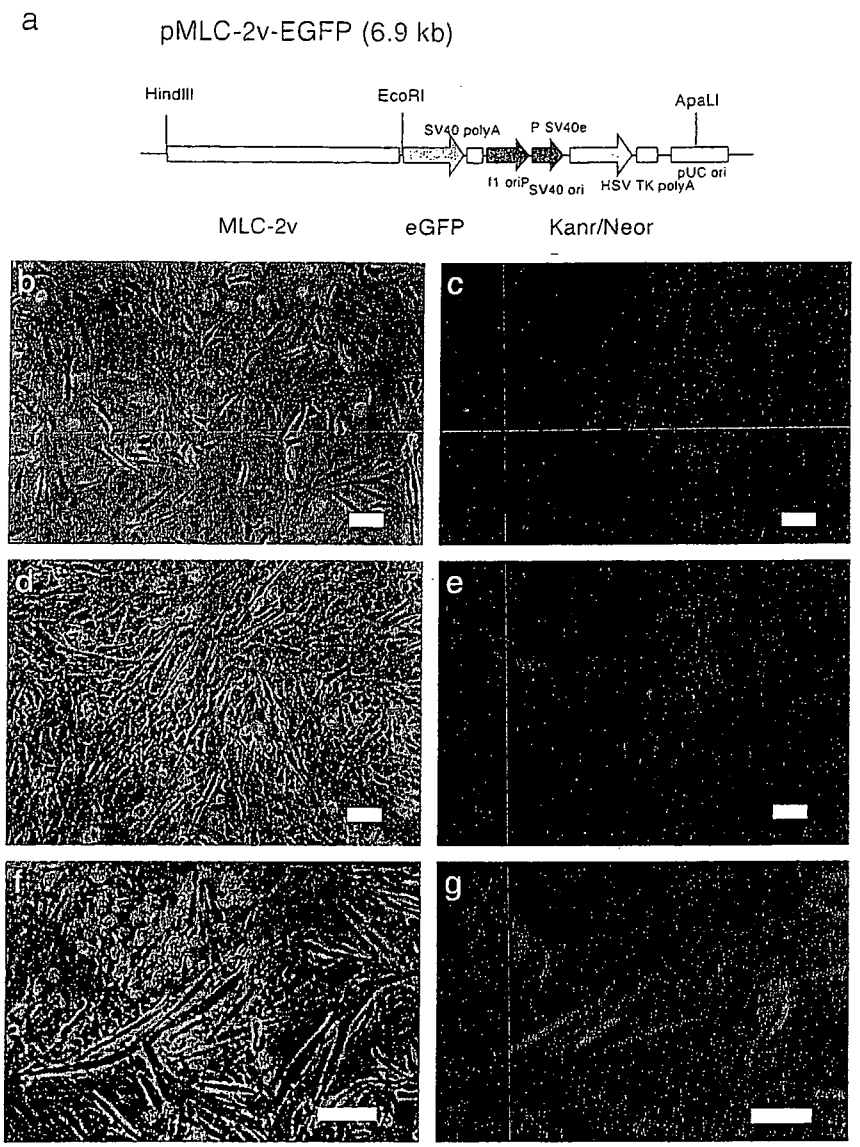

Fig. 1. Construction of pMLC-2v-EGFP and expression of EGFP in differentiated CMG cells. (a) Restriction map of pMLC-2v-EGFP. (b–g) Microscopy of the pMLC-2v-EGFP stably transfected CMG cells. b, d, and f shows phase contrast microscopy of the CMG cells after differentiation, and c, e, and g represent fluorescent microscopic views of the same field in b, d, and f. (b, c) 3 days, (d, e) 7 days, and (f, g) 4 weeks after the 5-azacytidine exposure. Bars indicate 100 μm.

with PBS containing Adex-LacZ virus at 10 MOI for 100 min. The cells were washed three times to remove virus remaining on the cell surface. Prior to transplantation, the cells were incubated in IMDM with 20% FBS for 2 days.

2.6. Transmission electron microscopy

Cells were washed three times with PBS (pH 7.4) prior to transmission electron microscopy. Cells were initially fixed with PBS containing 2.5% glutaraldehyde for 2 h. The cells were then embedded in epoxy resin. Ultra-thin sections cut horizontally to the growing surface were double stained in uranyl acetate and lead citrate, and viewed under a JEM-1200EX transmission electron microscope.

2.7. Bromodeoxyuridine (BrdU) incorporation

To detect nuclei undergoing DNA synthesis, cells were incubated with BrdU (10 μM) for 5 h, rinsed with PBS, and then fixed in methanol for 20 min at 4 °C. Immunofluorescence microscopy using a monoclonal antibody against BrdU was performed as described previously [14]. The percentage of BrdU-positive cells was estimated by counting cells on photographs of randomly chosen fields.

2.8. Gene expression analysis

Total RNA was extracted from EGFP(+) cells isolated at 7 days following transfection. RT-PCR was performed to detect α-myosin heavy chain (MHC), β-MHC, α-

skeletal actin, α-cardiac actin, myosin light chain-2v (MLC-2v), MLC-2a, Cav1.2, myoD, calponin, and α-smooth muscle actin genes. The primers and PCR cycles used were as described previously [6,15,16]. Primers for Cav1.2 were CTGCAGGTGATGATGAGGTC for the forward primer and GCGGTGTTGTTGGCGTTGTT for the reverse primer.

2.9. Immunostaining

Cells were attached to gelatin-coated glass slides, fixed in 4% paraformaldehyde, and then stained with primary antibodies against anti-GATA4, anti-troponin I, and anti-MEF2C antibodies (all from Santa Cruz Biotechnology), or anti-connexin43 antibody (Sigma). Anti-goat-IgG conjugated with Texas red or anti-rabbit IgG conjugated with Rhodamine (1:500, Pharmingen) was use as a secondary antibody.

2.10. Action potential recording

Electrophysiological studies were performed in IMDM containing (mmol/L) $CaCl_2$ 1.49, KCl 4.23, and HEPES 25 (pH 7.4). Cultured cells were placed on the stage of an inverted phase contrast optic (Diaphoto-300, Nikon) at 23 °C. Action potentials were recorded using conventional microelectrodes as described previously [8]. Intracellular recordings were taken from MLC2v-EGFP-purified cells 3 weeks following transfection.

2.11. Cell transplantation

Animal Care and Use Committees of Keio University approved all experimental procedures and protocols. Female scid mice (12 weeks) were anesthetized initially with ether and placed on a warm pad maintained at 37 °C. The trachea was cannulated with a polyethylene tube connected to a respirator (Shinano, Tokyo, Japan) with a tidal volume set at 0.6 ml and a rate set at 110/min. Mice were then anesthetized with 0.5–1.5% isoflurene under controlled ventilation with a respirator for the remainder of the surgical procedure. A left thoracotomy was performed between ribs 4 and 5, and the pericardial sac was removed. Isolated EGFP(+) cells that had been expanded for 5 days were resuspended in PBS at a concentration of 5×10^7 cells/ml. A total cell suspension volume of 50 μl was drawn into a 50 μl Hamilton syringe with a 31-gauge needle, and 10 μl was injected into the anterior wall of the left ventricle. Following the transplantation, residual cells in the syringe were collected and stained with trypan blue. The total and living cell numbers were counted. The number of living cells to inject was calculated by the following formula. (The injected living cells)=[(Total injected cells)−(Residual cells in the syringe)](Percent of living cells). Injection of PBS was used as a control.

2.12. Histological studies

The mice were sacrificed, and the hearts were dissected and fixed in 2% formaldehyde and 0.2% glutaraldehyde in PBS at room temperature for 5 min. The hearts were then washed in PBS and then incubated overnight in X-gal solution (1 mg/ml X-gal, 15 mmol/L potassium ferricyanide, 15 mmol/L potassium ferrocyanide, and 2 mmol/L $MgCl_2$ in PBS). The hearts were refixed in the same fix solution, embedded in paraffin, and sectioned into 6-μm-thick slices for hematoxylin–eosin staining. The numbers of X-gal-stained CMG cells were counted using serial sections of the transplanted heart (more than 200 slices/mouse), and an estimate of total transplanted cell survival was obtained using the following formula. (Percent of cells surviving in the recipient heart)=[(Total surviving cells in the recipient heart)/(Injected living cells)]100.

To observe EGFP fluorescence, the hearts were embedded in OCT compound and frozen with liquid nitrogen. A cryostat was used to generate 6-μm-thick sections. The samples were examined with a confocal LASER microscope (LSM510; Carl Zeiss, Jena, Germany). The GFP signal was confirmed by emission finger printing, using the LSM 510 Meta spectrometer (Carl Zeiss).

2.13. Electrocardiography (ECG) recording

ECG recordings were performed 2 and 4 weeks after transplantation. Mice were anesthetized with ether, needle limb leads were fixed, and the ECG was recorded for 1 h.

2.14. Statistics

Values are presented as mean±SD. The significance of differences among mean values was determined by ANOVA. Statistical comparison of the control and treated groups was carried out using the nonparametric Fisher's multiple comparison tests. The level accepted for significance was $p<0.05$.

3. Results

3.1. Regenerated cardiomyocytes, but not other cell types, express EGFP

G418-resistant cells were exposed to 5-azacytidine and after 3 days EGFP(+) cells exhibited a fibroblast-like morphology (Fig. 1b,c), and were difficult to distinguish from other cell types. After 7 days, the EGFP(+) cells displayed a spindle-like morphology (Fig. 1d,e), but did not spontaneously beat at this stage. After 3 weeks, the EGFP(+) cells began to appear more rod-like and form inter-cell connections and after 4 weeks spontaneous beating was observed (Fig. 1f,g). Some fractions of the EGFP(−)

cells differentiated into adipocytes, but other EGFP(−) cells did not display any specific morphology. These findings indicate that the MLC2v–EGFP system may be a useful method for distinguishing regenerated cardiomyocytes from other cell types at an early stage.

3.2. Fluorescence-activated cell sorting (FACS) analysis

FACS analysis was performed 3 day after 5-azacytidine exposure to isolate regenerated cardiomyocytes. Control cells (before 5-azacytidine exposure) showed no detectable fluorescence (Fig. 2a), whereas 3 days after 5-azacytidine exposure the cells stable transfected with the MLC2v-EGFP expression plasmid generated sufficient EGFP signal for cell sorting (Fig. 2b). The EGFP(+) fraction ranged from 6–24%. Fig. 2c,d shows the cells 4 days after cell sorting (7 days after 5-azacytidine exposure) displaying a fibroblast-like morphology. The percentage of EGFP-positive cells was calculated by comparing cell counts from phase contrast microscopy with EGFP(+) cell counts using fluorescence microscopy, 3 days after cell sorting. More than 99% of the sorted cells expressed EGFP fluorescence. After 3 weeks, these cells had a spindle-like appearance and began spontaneous beating (Fig. 2e,f).

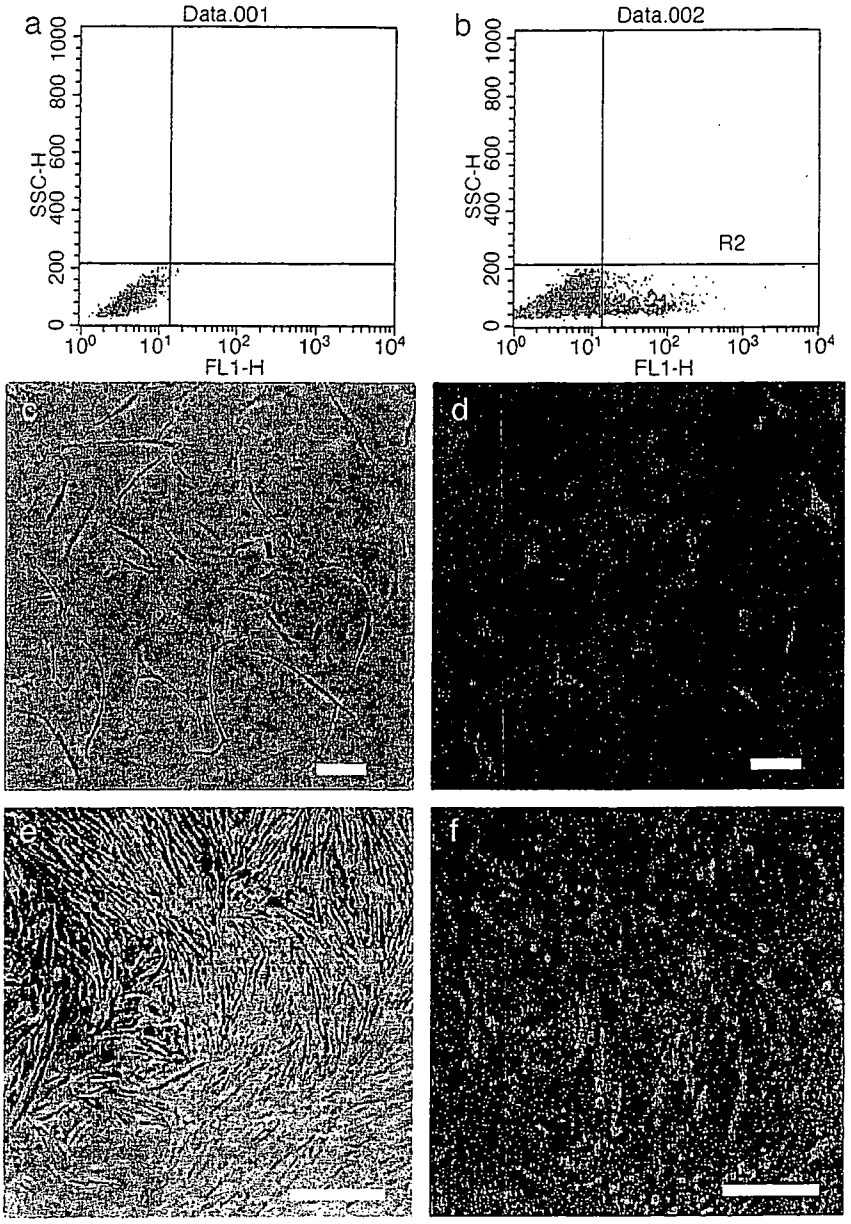

Fig. 2. FACS analysis of the pMLC-2v-EGFP-transfected cells and microscopy of the sorted cells. (a, b) FACS analysis of the pMLC-2v-EGFP-transfected cells. The horizontal axis indicates the intensity of EGFP fluorescence. (a) Control cells, (b) cells 3 days after exposure to 5-azacytidine exposure. d and f are fluorescence microscopy images of the EGFP signal. c and e are phase contrast microscopy views of the same field. (c, d) 4 days, and (e, f) 3 weeks after cell sorting. Note that all the cells display EGFP fluorescence, and that the EGFP(+) CMG cells exhibit a cardiomyocyte-like appearance and spontaneously beat after 3 weeks. Bars in c,d and e,f indicate 100 and 500 μm, respectively.

3.3. Character of the sorted EGFP(+) regenerated cardiomyocytes

A total of 768 single EGFP(+) cell clones were isolated using FACS analysis. Although EGFP(+) cells undergo cell division after 5-azacytidine exposure, a cardiomyocyte cell line could not be generated as cells stop proliferating after several cell divisions. The cells were exposed to BrdU to confirm their mitogenicity, and double immunostaining was performed with antisarcomeric myosin and anti-BrdU antibodies. Myosin-positive cells incorporated BrdU until day 5, but stopped incorporating it after day 7 (Fig. 3a). This finding shows that the mitogenicity of the isolated EGFP(+) CMG cells is limited, so it can be assumed that the risk of cardiomyosarcoma formation is negligible.

RT-PCR analysis of cardiac contractile proteins revealed that the isolated EGFP(+) CMG predominantly express the β-myosin heavy chain, α-skeletal-actin, and MLC-2v, indicating that the phenotype of these cells represents fetal ventricular cardiomyocytes. These cells also express cardiac L-type Ca^{2+} channels but did not express myogenic genes such as myoD, or smooth-muscle-specific genes, such as calponin or α-smooth muscle actin genes (Fig. 3b).

3.4. Action potential recording

MLC2v-EGFP-selected cells showed regular spontaneous beating 3 weeks following selection. The action potentials of these cells had a relatively shallow resting membrane potential with a late diastolic slow depolarization, like a pacemaker potential. They also displayed peak-notch-plateau characteristics representative of ventricular cardiomyocyte-like action potentials (Fig. 3c).

3.5. Immunostaining and transmission electron microscopy

Immunostaining revealed that EGFP(+) but not EGFP(−) CMG cells express cardiac troponin I (Fig. 4a–d). EGFP(+) CMG cells express both GATA4 and MEF2C, respectively (Fig. 4e,f). Interestingly, EGFP(−) CMG cells express GATA4 and Nkx2.5. These findings are consistent with the previous report that these cardiac transcription factors are expressed before final 5-azacytidine exposure [6]. EGFP(+) CMG cells also express connexin43 (Fig. 4g).

The sorted GFP(+) cells were cultured for 2 weeks, fixed, and processed for transmission electron microscopy. The typical contractile apparatus of the sarcomeres, including striation pattern, was observed (Fig. 4h).

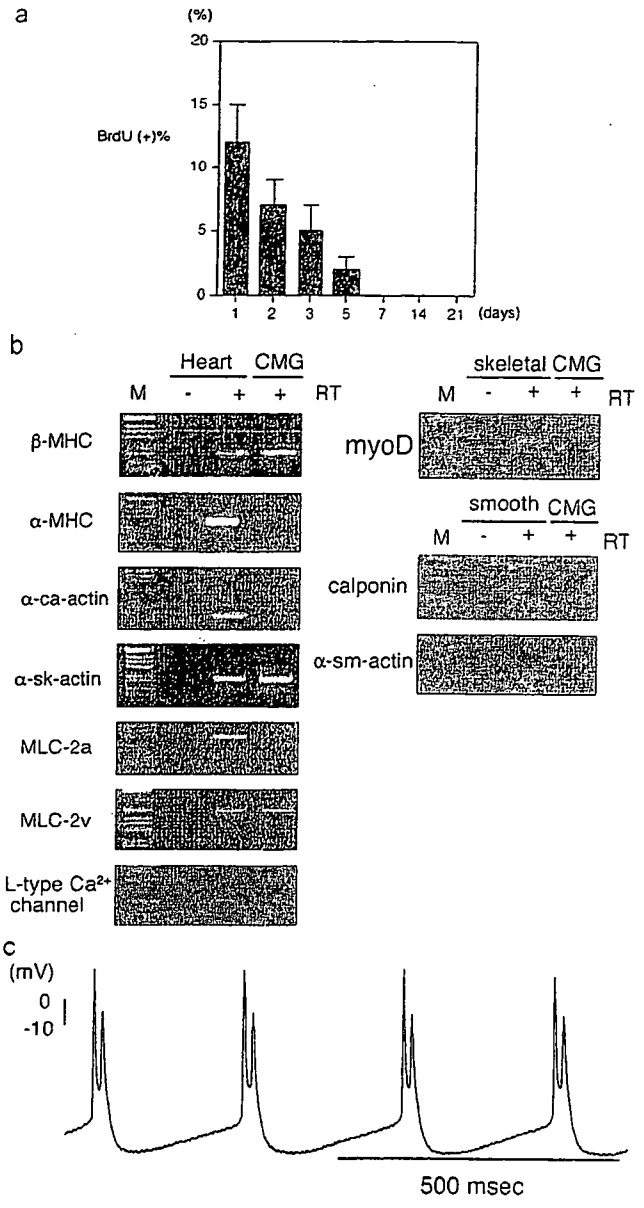

Fig. 3. Characteristics of the sorted CMG cardiomyocytes. (a) BrdU incorporation of EGFP(+) CMG cells after cell sorting. BrdU was loaded for 5 h, and its incorporation was detected. BrdU incorporation was observed until 5 days after cell sorting (8 days after 5-azacytidine exposure). (b) Phenotype of the EGFP(+) CMG cells. RT-PCR was performed for α-MHC, β-MHC, MLC-2v, MLC-2a, α-skeletal actin, α-cardiac actin, and cardiac α1c Ca^{2+} channel. The expression pattern of the cardiac contractile protein indicated that these cells had the fetal ventricular phenotype. MLC-2v-EGFP selected cells did not express myoD, calponin, and α-smooth muscle actin genes. Femoral muscle, which includes vascular smooth muscle cells, were used as a positive control. M: 1-kb DNA ladder. RT: reverse transcription. (c) The representative tracing of the action potentials at 3 weeks after cell sorting was shown. These action potentials show ventricular cardiomyocyte-like action potentials.

3.6. Cell transplantation study

Animals with transplanted EGFP(+) cells were sacrificed at 2, 4, 8, and 12 weeks. Confocal LASER microscopy revealed that the EGFP(+) transplanted cardiomyocytes survived in the recipient heart (Fig. 5a–c). The control experiment revealed no EGFP(+) transplanted cardiomyocytes (data not shown) [17]. The orientation of the transplanted cells was consistent with the cardiomyocytes of the recipient heart. The EGFP(+) cells were observed only at the site of injection in the left ventricle and in no other parts of the heart. We also confirmed that these green signals were

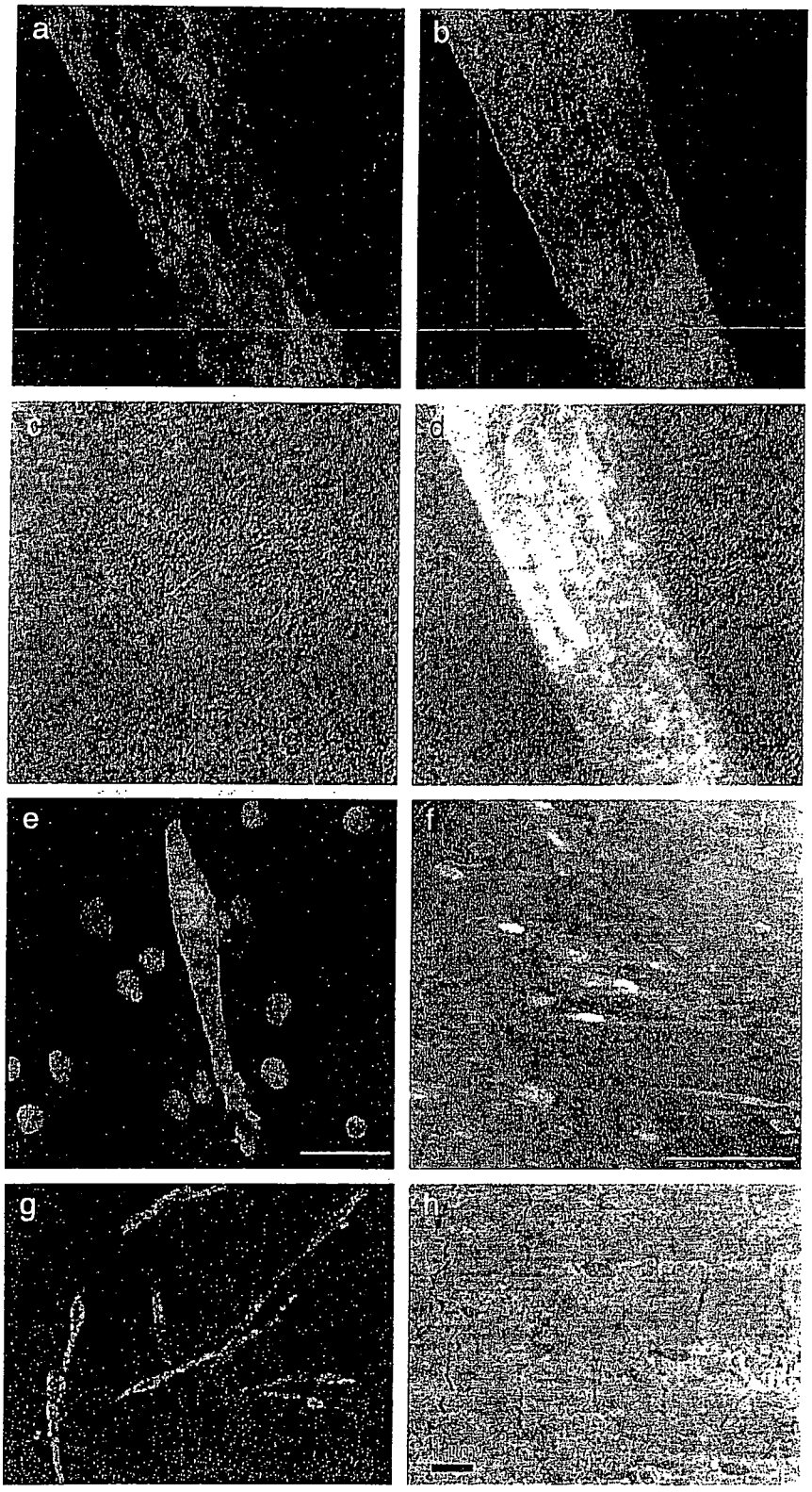

Fig. 4. Photograph of immunofluorescence and transmission electron micrograph of CMG cells. (a–d) EGFP(+) and EGFP(−) CMG cells were stained with anti-troponin I antibodies (a) and DAPI (c). EGFP(+) CMG cells expressed troponin I, but EGFP(−) CMG cell did not express troponin I. (e) Immunofluorescent staining with GATA4. Both EGFP(+) and EGFP(−) CMG cells expressed GATA4. (f) Immunofluorescent staining with MEF2C. Both EGFP(+) and EGFP(−) CMG cells expressed MEF2C. (g) Immunofluorescent staining with connexin43. EGFP(+) CMG cells expressed connexin43. (h) Transmission electron microscopy of the CMG cells showed typical contractile apparatus.

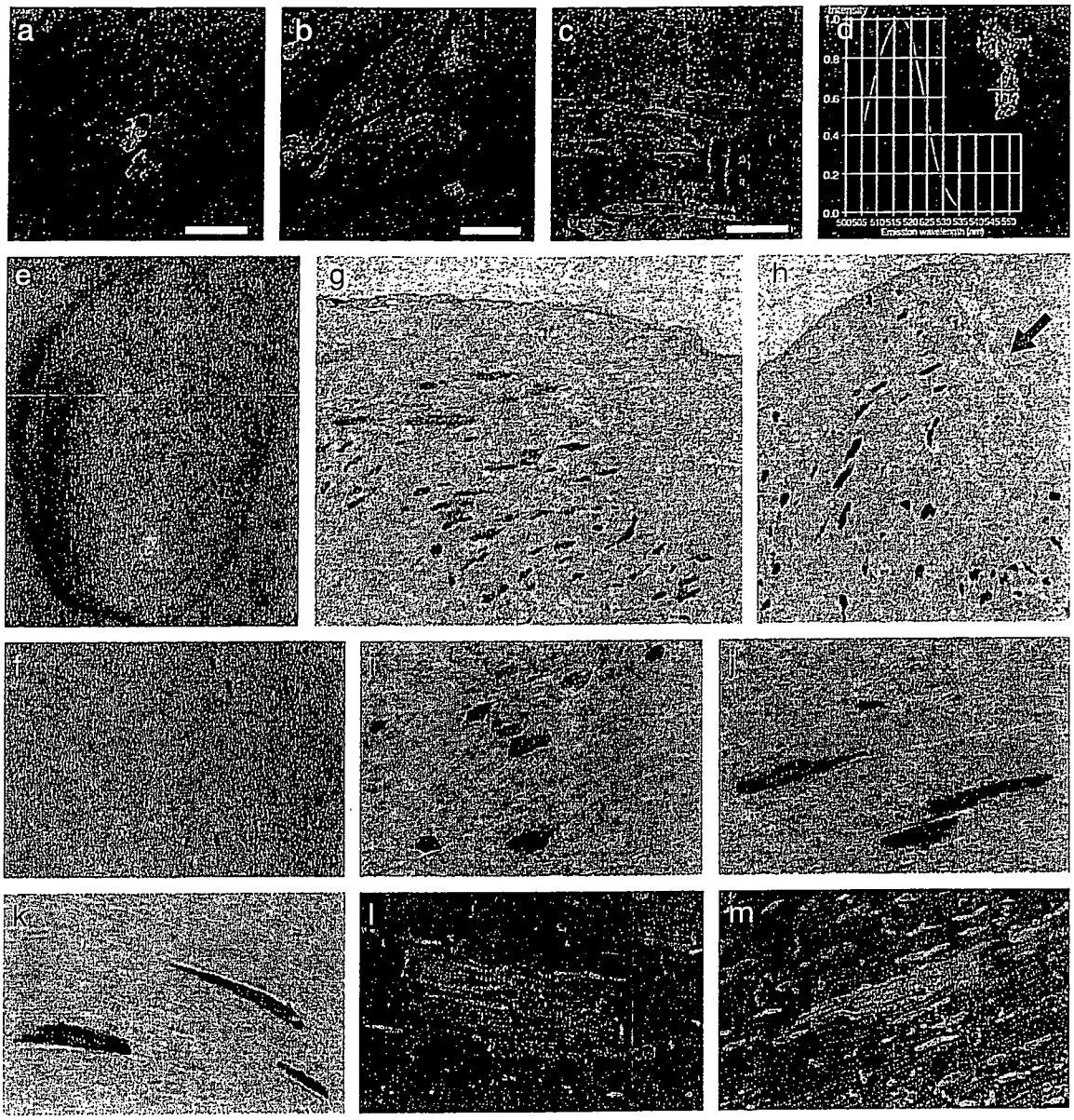

Fig. 5. Histological analysis of the transplanted CMG cells. (a–c) Confocal microscopy of the recipient heart transplanted with the sorted cardiomyocytes at 4 weeks. The transplanted cells could be clearly identified by EGFP signals. a and b show the transverse section of the transplanted cardiomyocytes, and c shows the longitudinal section. Bars indicate 50 μm. (d) The emission profile of the green signal in GFP^+ cells was investigated by CLSM. The emission peak existed at 510–530 nm, and the profile was ascertained to be that of GFP, and not arising from nonspecific background. The inset shows the GFP^+ transplanted cells, and the cross indicates the site of the emission profile. (e–m) The bone-marrow-derived cardiomyocytes were sorted and marked with adenovirus-mediated LacZ gene. e is a photograph of the whole heart, and f shows an enlarged photograph of the injected site. The transplanted LacZ-positive cells were identified from the surface. g and h show the microscopy of the injected site of the left ventricle. The samples were stained with LacZ and hematoxylin–eosin. i–k show higher magnification of the same fields: i shows the transverse section, and j,k show the longitudinal section. (l, m) Transplanted CMG cells were stained with anticonnexin43 antibody and DAPI. Connexin43 was expressed at the both ends of the transplanted EGFP(+) CMG cells. Green: EGFP, Blue: DAPI, Red: connexin43.

not due to nonspecific background fluorescence, but due to the EGFP itself, using absorbance frequency analysis on a LSM510 Meta spectrometer (Fig. 5d).

Fig. 5e shows the entire murine heart stained with LacZ at 4 weeks after transplantation, and Fig. 5f showed an enlarged photograph of the site of injection. Cells were transplanted into the anterior free wall of the left ventricle and were observed to be rectangular in shape and located at the surface of the heart. Fig. 5g,h shows the site of injection in a transverse section of the left ventricle stained with LacZ and hematoxylin–eosin 4 weeks after transplantation. The scar of the injection needle is shown in Fig. 5h. Granulomatous tissue was also observed around the site of injection. The LacZ-stained transplanted cells were clearly visible, and were located throughout the site of injection. Fig. 5i–k shows transverse and longitudinal sections of the transplanted cardiomyocytes at higher magnifications. This figure clearly shows the arrangement of the transplanted

cells parallel to the cardiomyocytes of the recipient heart. Fig. 5l,m shows expression of connexin43 at the longitudinal border between transplanted EGFP(+) CMG cells and adjacent cardiomyocytes of the recipient heart.

Transplanted cardiomyocytes survived in the recipient heart for more than 3 months and the estimated percentage of cells surviving transplantation was 6.5±3.2%. Table 1 shows the diameter of transplanted cardiomyocytes in transverse section. The diameter increased to almost the same size as the cardiomyocytes in the recipient heart over 4 weeks after which time no further increase was observed.

3.7. ECG recording and survival curve

Of the 35 mice that had undergone cell transplantation, 5 died within 24 h. This is most likely a result of the surgical procedure. The remaining 30 mice survived the duration of the observation period. ECGs recordings in 5 mice at 2 and 4 weeks, respectively, showed no evidence of arrhythmia (ventricular premature beats, ventricular tachycardia) during the recording period (data not shown). This finding suggests that survival of recipients in this model is not affected by arrhythmia.

4. Discussion

Since our report that cardiomyocytes can be regenerated from bone marrow stem cells [6,7], several studies have shown that transplantation of bone-marrow mononuclear cells or bone marrow stem cell fractions into the heart can improve cardiac function. Although the direct transplantation of these cells omits prior differentiation or purification, and thereby shortens the therapeutic period, it remains undetermined whether transplanted cells differentiate into the desired cardiomyocytes or endothelial cells, and not into other cell types including osteoblasts, chondroblasts, or adipocytes. The establishment of a reliable method to repair injured myocardium using cardiomyocyte transplantation requires the preparation of a sufficient number of well-characterized, purified regenerated cardiomyocytes, and an estimation of the survival rate of the transplanted cells.

Tomita [18] reported that the transplantation of 5-azacytidine-treated primary cultured marrow-stromal cells improved the function of the infarcted myocardium. Since the population of mesenchymal stem cells in primary cultured mice marrow stromal cells is less than 0.01%, it is likely that most of the cells transplanted do not differentiate into cardiomyocytes, and that the observed improvement in cardiac function is caused by an improvement in ventricular remodeling or stimulation of angiogenesis.

Jackson transplanted adult stem cells [CD34(−)/low, c-Kit(+), Sca-1(+)] into lethally irradiated mice subsequently rendered ischemic by coronary artery occlusion followed by reperfusion, and reported that the engrafted cells migrated into ischemic cardiac muscle and blood vessels, differentiated to cardiomyocytes and endothelial cells, and contributed to the formation of functional tissue [19]. They found that the donor-derived endothelial cells were present at around 3.3%, primarily in small vessels adjacent to the infarct, and that donor-derived cardiomyocytes were present at around 0.02% and were found primarily in the peri-infarct region. Taken together, these findings show that differentiation from marrow stromal cells to cardiomyocytes in vivo is possible, but that their prevalence is less than other cell types. Condrelli [20] reported that neural stem cells differentiated into heart muscle cells when mixed with heart muscle cells from newborn rats in a process known as transdifferentiation. The mechanism of in vitro transdifferentiation is based on the idea that the developmental limitations of tissue specific stem cells are dictated by the environment, and that new signals that relax these limitations may be provided by cells from a different tissue [20].

It is most likely that the direct transplantation of stem cells into the heart does not facilitate their differentiation into cardiomyocytes, but merely results in their fusion with residual cardiomyocytes. We propose a more rigorous method to achieve repair of damaged tissue by first differentiation adult stem cells cardiomyocytes in vitro, and then transplanting a sufficient number of differentiated cardiomyocytes into the damaged heart tissue. To avoid possible adverse effects, we emphasize the importance of thoroughly investigating the molecular and electrophysiological characteristics of the stem cell-derived regenerated cardiomyocytes prior to transplantation.

In the present study, we used an EGFP reporter gene under the control of the MLC-2v promoter to tag isolated cardiomyocytes. Following FACS analysis, 99% of the isolated cardiomyocytes expressed EGFP, and when transplanted into the recipient heart they survived for at least 4 weeks. We observed no other cell types in the transplanted area, but this may have been because we only used a strongly expressing EGFP(+) fraction.

Table 1
Diameter of the transplanted bone-marrow-derived cardiomyocyte

Time after transplantation (weeks)	2	4	8	12	Recipient cardiomyocytes
Diameter (μm)	10.5±3.6*	19.0±4.8$	19.1±5.0$	19.1±4.9$	19.5±5.1

The diameter of the transplanted cardiomyocytes was measured by the transverse section of the recipient hearts. Each data was obtained by measuring 200 cells. Mean±SD. $: not significant vs. recipient cardiomyocytes.

* $p<0.01$ vs. 4 weeks and recipient cardiomyocytes.

A plasmid encoding reporter genes and cardiac specific gene promoters was used in a previous study to isolate cardiomyocytes from ES cells or embryonic carcinoma cells (EC cell) [21]. Klug et al. [8] transfected a fusion gene containing the α-myosin heavy chain (α-MHC) promoter and aminoglycoside phosphotransferase (NeoR) into pluripotent ES cells, then differentiated these cells in vitro prior to G418 selection. They reported high purification (>99%) and a survival period in the recipient heart of at least 7 weeks following transplantation. Zweigerdt et al. [22] and Zandstra et al. [23] reported a lab-scale protocol to generate cultures of highly enrich cardiomyocyte from ES cells transfected with a α-MHC-NeoR containing plasmid, and suggest its application to a larger-scale process for the supply of stem cell based cardiomyocytes. Muller et al. [9] isolated a subpopulation of ventricular-like cardiomyocytes from ES cells by transfecting the EGFP gene under the control of the MLC-2v promoter and cytomegalovirus enhancer. Moore et al. [24] reported that EC cell (P19Cl6)-derived cardiomyocytes could be isolated using an EGFP reporter under the control of 250 bp of the MLC-2v promoter. They enzymatically digested embryoid bodies, then isolated a population of cardiomyocytes (97% pure) using Percoll gradient centrifugation and FACS analysis. Kolossov et al. [25] reported the use of EGFP under the control of the cardiac α-actin promoter to isolate ES cell-derived cardiomyocytes. The present study confirmed the efficiency of this strategy for the isolation and purification of cardiomyocytes from bone-marrow-derived stem cells.

Reinecke and Murry [26] and Zhang et al. [27] highlighted the importance of a quantitative analysis of grafted cardiomyocytes, since a large number of fetal or neonatal cardiomyocytes often display apoptosis within several days of transplantation. They reported that only a small percentage of cardiomyocytes survive in the cryoinjured recipient heart, and that heat shock or adenoviral transfer of constitutive active Akt genes could increase their survival. In comparison, the present study reports a slightly higher survival rate for bone marrow-derived cardiomyocytes. One possible reason is the difference in the experimental models as the present study used a mouse uninjured model and not a rat cryoinjured heart model. Another reason is the small size of our not fully differentiated transplanted cells compared with fetal or neonatal cardiomyocytes. A small size may allow transplanted cells to go deep into the recipient heart without mechanical injury.

Recently, Takeda et al. [28] reported that the life span of human bone marrow mesenchymal stem cells could be prolonged by infecting the cells with the retrovirus encoding oncogene bmi-1, human papilloma virus E6 and E7, and human telomerase reverse transcriptase over 150 population doublings, and that these cells could be induced to differentiate into cardiomyocyte using 5-azacytidine and co-culture with the rat cardiomyocytes. Although this procedure is not suitable for clinical application at the present stage, the findings provide valuable information on the use of human bone marrow stem cells for the regeneration of cardiomyocytes.

In summary, the present study provides a new model for tissue engineering. Further studies are required to improve cardiomyocyte differentiation and to increase the efficiency of the transplantation procedure.

Acknowledgements

This study was supported in part by the research grants (10B-1) of "Nervous and Mental Disorders from the Ministry of Health and Welfare", Japan, the research grants from the Ministry of Education, Science and Culture, Japan, and the research grants from Health Science Research Grants for Advanced Medical Technology from the Ministry of Welfare, Japan.

References

[1] Leor J, Patterson M, Quinones MJ, Kedes LH, Kloner RA. Transplantation of fetal myocardial tissue into the infarcted myocardium of rat A potential method for repair of infarcted myocardium? Circulation 1996;94(Suppl. 9):II332–6.
[2] Matsushita T, Oyamada M, Kurata H, Masuda S, Takahashi A, Emmoto T, et al. Formation of cell junctions between grafted and host cardiomyocytes at the border zone of rat myocardial infarction. Circulation 1999;100(Suppl. 19):II262–8.
[3] Sakai T, Li RK, Weisel RD, Mickle DA, Kim EJ, Tomita S, et al. Autologous heart cell transplantation improves cardiac function after myocardial injury. Ann Thorac Surg 1999;68:2074–80.
[4] Weissman IL. Translating stem and progenitor cell biology to the clinic: barriers and opportunities. Science 2000;287:1442–6.
[5] Weissman IL, Anderson DJ, Gage F. Stem and progenitor cells: origins, phenotypes, lineage commitments, and transdifferentiations. Annu Rev Cell Dev Biol 2001;17:387–403.
[6] Makino S, Fukuda K, Miyoshi S, Konishi F, Kodama H, Pan J, et al. Cardiomyocytes can be generated from marrow stromal cells in vitro. J Clin Invest 1999;03:697–705.
[7] Hakuno D, Fukuda K, Makino S, Konishi F, Tomita Y, Manabe T, et al. Bone marrow-derived cardiomyocytes (CMG cell) expressed functionally active adrenergic and muscarinic receptors. Circulation 2002;105:380–6.
[8] Klug MG, Soonpaa MH, Koh GY, Field LJ. Genetically selected cardiomyocytes from differentiating embryonic stem cells form stable intracardiac grafts. J Clin Invest 1996;98:216–24.
[9] Muller M, Fleischmann BK, Selbert S, Ji GJ, Endl E, Middeler G, et al. Selection of ventricular-like cardiomyocytes from ES cells in vitro. FASEB J 2000;14:2540–8.
[10] O'Brien TX, Lee KJ, Chien KR. Positional specification of ventricular myosin light chain 2 expression in the primitive murine heart tube. Proc Natl Acad Sci U S A 1993;90:5157–61.
[11] Henderson SA, Spencer M, Sen A, Kumar C, Siddiqui MA, Chien KR. Structure, organization, and expression of the rat cardiac myosin light chain-2 gene. Identification of a 250-base pair fragment which confers cardiac-specific expression. J Biol Chem 1989;264:18142–8.
[12] Kanegae Y, Makimura M, Saito I. A simple and efficient method for purification of infectious recombinant adenovirus. Jpn J Med Sci Biol 1995;47:157–66.
[13] Niwa H, Yamamura K, Miyazaki J. Efficient selection for high-expression transfectants by a novel eukaryotic vector. Gene 1991;108:193–200.